Nonreciprocal microwave devices based on magnetic nanowires

Bijoy K. Kuanr,[1] V. Veerakumar,[1] Ryan Marson,[2] Sanjay R. Mishra,[2] R. E. Camley,[1,a)] and Z. Celinski[1]
[1]*Center for Magnetism and Magnetic Nanostructures, University of Colorado, Colorado Springs, Colorado 80918, USA*
[2]*Department of Physics, University of Memphis, Memphis, Tennessee 38152, USA*

(Received 16 March 2009; accepted 5 April 2009; published online 20 May 2009)

We use magnetic nanowires in an alumina matrix as the active element in microwave nonreciprocal resonance isolators. The design is related to waveguide *E*-plane isolators but is planar and much smaller than typical waveguide isolators. There is a nonreciprocal attenuation of the wave in forward and reverse directions. The isolation is about 6 dB/cm at 23 GHz. The bandwidth of the device is relatively large (5–7 GHz) in comparison to ferrite-based devices. The central frequency of the device can be tuned with the application of magnetic field. © *2009 American Institute of Physics*. [DOI: 10.1063/1.3124657]

Reciprocal devices such as phase shifters and band-stop filters are common signal processing elements and have been constructed using both ferrites and metallic films.[1–4] However, nonreciprocal devices, such as isolators, have only been constructed with ferrites.[1,2] An isolator is a two-port device that allows wave propagation in one direction but has significant attenuation for propagation in the reverse direction. The scattering matrix of an ideal two-port isolator is given by

$$S = \begin{vmatrix} S_{11} & S_{12} \\ S_{21} & S_{22} \end{vmatrix} = e^{i\theta} \begin{vmatrix} 0 & 0 \\ 1 & 0 \end{vmatrix}. \quad (1)$$

In an ideal isolator both the ports (1 and 2) are matched, but transmission occurs only in the forward direction and the reverse transmission is blocked.

Isolators typically operate in a frequency range that depends on an external magnetic field H_0 and on the saturation magnetization ($4\pi M_S$). Because ferrites are typically characterized by a low saturation magnetization, their operating frequencies are generally below 10 GHz for small magnetic fields. Furthermore, ferrite isolators are generally bulky, with dimensions on the order of a few centimeters. The frequency range can be increased by using ferromagnetic metals[3] because of their high $4\pi M_S$ ($4\pi M_S$ is 6.1 kG for Ni and 21.5 kG for Fe). However, the presence of a metal introduces eddy currents, resulting in energy losses that significantly damp electromagnetic waves. In this investigation we use a hybrid structure that combines the larger $4\pi M_S$ of ferromagnetic nickel nanowires[5–8] in an alumina dielectric matrix to reduce eddy currents. These features allow the creation of a high-frequency nonreciprocal device.

The Ni nanowires were electrodeposited in a hole-pattern of commercial anodized alumina templates of 60 μm in thickness and 150 nm in pore size. To accomplish this, the alumina template was first painted with a gallium-indium eutectic (Aldrich) on one side to allow for electrical conduction. The painted side was placed in contact with a copper plate (32×51 mm^2). The copper plate was partially covered with electrical tape to prevent any unwanted deposition. The exposed part of the plate was used for making electrical contact. The copper plate along with the attached template was submerged in a nickel plating solution which completely covered the top of the membrane. For the anode, a nickel wire (99.98% pure) of 1.0 mm diameter was used. Electrodeposition was carried out using a potentiostat at 1.5 V and a constant current of 100 mA. The deposition time was varied to control the lengths of the nanowires. Transmission electron microscopy (TEM) imaging showed the typical diameter of the wires was 150 nm.

The monolithic microwave devices were fabricated on top of the alumina templates filled with Ni nanowires. A thick layer of Cu ($\sim$1.5 μm) was deposited by dc magnetron sputtering. Photolithography and etching techniques were used to define a coplanar waveguide (CPW) transmission line structure, as shown in Fig. 1. The isolator is designed using the general ideas found in waveguide-based *E*-plane resonance isolators. The positioning of the nanowires for maximum isolation is observed to be at one side of the gap between the central signal line and the ground line of the CPW. This is achieved by multiple photolithography and etching procedures. The device characterization was done using a vector network analyzer along with a microprobe station. The frequency was swept from 0.05 to 70 GHz at a fixed external magnetic field (H). Noise, delay due to uncompensated transmission line connectors, its frequency dependence, and crosstalk which occurred in measurement data, have been taken into account by performing through-open-line calibration using NIST MULTICAL® software.[9]

The width of the signal lines was 20 μm and the length of the device was 3 mm. The filters were designed for a 50 Ω characteristic impedance.[10] The exact resonance fre-

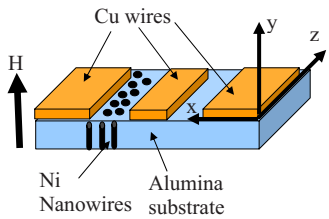

FIG. 1. (Color online) Schematic design of isolator and coordinate system. Nanowires are only on one side of the gap between the signal line and the ground line of the alumina matrix.

a)Electronic mail: rcamley@uccs.edu.

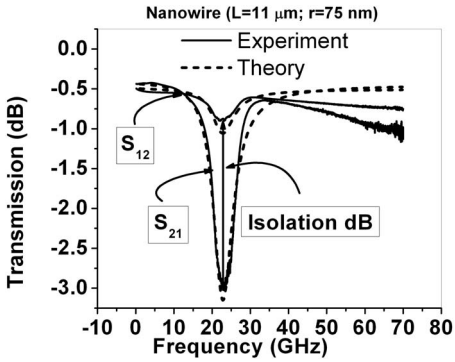

FIG. 2. Transmission response measured by the Network Analyzer system demonstrating the effect of isolation between ports 1 and 2 of the device measured at 5.6 kOe. The vertical line shows the level of isolation.

quency (f_r) was obtained from Lorentzian fits to the experimental transmission (S_{21}) data.

The transmission of the electromagnetic wave propagating from port 1 to 2 (S_{21}) as a function of frequency and measured at 5.6 kOe is shown in Fig. 2. The transmission in the forward direction is significantly reduced at the ferromagnetic resonance of Ni, while in the return direction from port 2 to 1 (S_{12}) the attenuation of the signal is small. The difference between these two values represents the degree of isolation and should be as high as possible. Results on the transmission coefficients show a nonreciprocal effect, which is about 6.5 dB/cm at 24 GHz. Figure 2 also shows a theoretical fitting which will be discussed below.

The bandwidth of the device is relatively large (5–7 GHz) in comparison to typical ferrite-based devices. Thus the device can operate over a wide frequency band (Fig. 3). The frequency tunability of the device is shown in Fig. 3(a) as a function of applied dc magnetic field. The solid line in Fig. 3(a) is obtained from the theoretical fittings.[11] Figure 3(b) shows the degree of isolation as a function of operating frequency.

One advantage of this geometry is that the full height of the nanowire can be easily biased by an external permanent magnet.[11] The second advantage of our device is that it has a

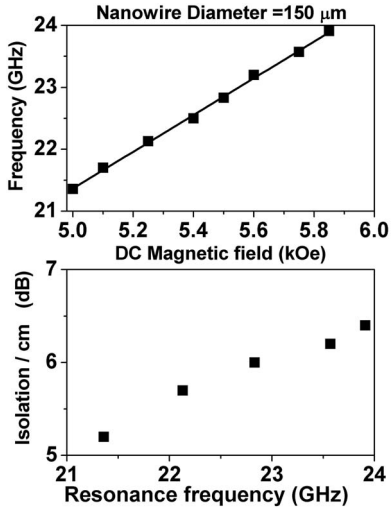

FIG. 3. (a) Operating frequency vs applied dc magnetic field. (b) Observed isolation as a function of frequency for the nanowire based coplanar structure. The magnetic field is changed by about 1 kOe over this frequency range.

much broader bandwidth (~6 GHz), in comparison to ferrite-based isolators which have a bandwidth of a few hundred megahertz. The bandwidth of the device is dictated primarily by the ferromagnetic resonance linewidth of the material, and Ni has a much larger linewidth in comparison to ferrites and garnets. The third advantage of the metallic based isolator over ferrite-based isolators is that it is better suited for high power microwave applications. This is because the power-handling capability of a ferromagnetic metal[12]—such as Ni—is much higher than yttrium iron garnet or spinel ferrites. The disadvantage of our device is the low value of the stop-band rejection (~9 dB/cm). This can be improved by using a microstrip transmission line geometry instead of the coplanar one that is being used here.

The performance of broadband isolators can be characterized by the ratio f_{max}/f_{min}, where f_{min} and f_{max} are defined as the edges of the frequency band in which the devices have acceptable operating characteristics. For the most advanced isolators available today this ratio is approximately 3:1. The measured broadband performance of our design is about 2.5:1. This does not represent any fundamental limitation on this ratio, but is due to the unavailability of a larger magnetic field in our laboratory. As the device under present study operates in a quasi-TEM mode, there is no cutoff frequency in the device. A much higher operating frequency (f_{max}) can be achieved by the use of a larger magnetic field. Furthermore the necessary applied fields will be lower than those used in ferrite isolators.

We have used a simple method to calculate the transmission parameter in the Ni nanowire isolator. The Ni nanowire/dielectric matrix structure is modeled by considering an effective medium with an effective susceptibility tensor. In the calculation, the wires have a radius $r=75$ nm with an interwire distance of $d=443$ nm. The large spacing between wires means that the wires are nearly noninteracting. The Ni nanowire/dielectric matrix can be approximated by an effective medium with the permeability components written as[13,14]

$$\mu_{\text{eff}} = (1-q)\mu_d + q\mu, \tag{2a}$$

$$\kappa_{\text{eff}} = q\kappa, \tag{2b}$$

where q is the volume fraction of the nanowires in the matrix, i.e., $q=\pi r^2/d^2$. The volume fraction $q \approx 0.09$ for our geometry. μ is the diagonal element of the permeability tensor for the nanowires, κ is the off-diagonal element of the permeability, and $\mu_d=1$ is the magnetic permeability of the dielectric medium.

For a nanowire magnetized in the longitudinal direction (along the y axis in the present case, see Fig. 1) the components of the permeability tensor are written as

$$\mu = 1 + \frac{4\pi\omega_M\omega_x}{\omega_0^2 - \omega^2}, \tag{3a}$$

$$\kappa = \frac{4\pi\omega_M\omega}{\omega_0^2 - \omega^2}, \tag{3b}$$

$$\omega_0^2 = \omega_x\omega_y, \quad \omega_{x,y} = (\omega_H + \mathrm{N}_{y,x}\omega_M). \tag{3c}$$

Here $\omega_H = \gamma H_0 - i\Gamma/2$, $\omega_M = 4\pi M_s\gamma$, γ is the gyromagnetic ratio, $4\pi M_s$ is the saturation magnetization, ω is the angular frequency, and H_0 is the external applied field. Here the line

width $\Gamma=(\Delta H_0+\alpha\omega/\gamma)$ where $\Delta H_0=2.5$ kG is the ferromagnetic resonance linewidth at zero frequency, and $\alpha=0.001$ is a parameter which determines how much the linewidth changes with frequency. N_x and N_y are the demagnetization factors of the wire with $N_x=N_y=2\pi$ and hence the resonance frequency $\omega_0=\omega_H+H_d$ where $H_d=2\pi\omega_M$.

The above discussion is only for a single nanowire. In the case of a nanowire assembly, the wire sees the external field and its own demagnetizing field but also the field created by the neighboring wires. With a finite structure there are additional demagnetizing terms coming from the top, bottom, and sides of the whole structure.[7] This shifts the resonance frequency of the single wire by setting $H_d=2\pi\omega_M(1-3q)$.[7]

The power transmitted per unit area in the CPW is calculated from the Poynting vector using the rf field components at all positions around the signal line in the waveguide. The power absorbed by the Ni-nanowire matrix is given by the relation $P=i\omega/2\ \mathrm{Re}(h_x^*M_x+h_z^*M_z)$, where h_x and h_z are the components of the rf field along the appropriate coordinate axes. Here $M_x=\chi_{\mathrm{eff}}^{xx}h_x+\chi_{\mathrm{eff}}^{xz}h_z$ and $M_z=\chi_{\mathrm{eff}}^{zx}h_z+\chi_{\mathrm{eff}}^{zz}h_x$, χ_{eff}^{xx}, χ_{eff}^{xz}, χ_{eff}^{zx}, and χ_{eff}^{zz} are the components of the susceptibility tensor of the effective medium which is calculated from Eq. (2). The power transmitted in the dielectric and air can be calculated from the relation $\langle P\rangle=(c/8\pi\sqrt{\varepsilon_{d,a}})(\vec{h}_{d,a}^*\bullet\vec{h}_{d,a})$, where ε_d and ε_a are the relative permittivity of the dielectric medium and air, respectively. Using the law of conservation of power we can find the transmission coefficient.[15]

The dotted lines in Fig. 2 show the results of the theoretical calculation for the transmission which are very close to the experimental data. We can obtain some insight into the behavior, by using earlier work on resonance isolators in waveguides. In this case, the maximum isolation can be obtained by placing the magnetic material at a position where the ellipticity factor $\xi=|h_z/h_x|=1$. The experimental curves at 23 GHz correspond to $\xi=0.65$ which is obtained when the edge of the nanowires structure is at a distance of 6 μm from the center of the signal line as in the experiment. From our calculations we find that the largest nonreciprocity in this structure would occur if the edge of the nanowires were at a distance of 15 μm from the signal line. This would correspond to an ellipticity factor of 0.91.

In summary, we have designed, fabricated, and characterized a nonreciprocal microwave planar isolator using high aspect ratio Ni nanowires, made by electrodeposition inside the pores of an alumina matrix. The isolation of the device reaches ~6.5 dB/cm at 24 GHz with a bandwidth of ~6 GHz. This device has several advantages over typical ferrite-based resonance isolators.

The work at UCCS was supported by DOA under Grant No. W911NF-04-1-0247.

[1] D. M. Pozar, *Microwave Engineering*, 2nd ed. (Wiley, New York, 1998).
[2] I. Huynen, G. Goglio, D. Vanhoenacker, and A. Vander Vorst, IEEE Microw. Guid. Wave Lett. **9**, 401 (1999).
[3] B. K. Kuanr, Z. Celinski, and R. Camley, Appl. Phys. Lett. **83**, 3969 (2003).
[4] U. Ebels, J.-L. Duvail, P. E. Wigen, L. Piraux, L. D. Buda, and K. Ounadjela, Phys. Rev. B **64**, 144421 (2001).
[5] J.-E. Wegrowe, D. Kelly, A. Franck, S. E. Gilbert, and J.-Ph. Ansermet, Phys. Rev. Lett. **82**, 3681 (1999).
[6] I. Dumitru, F. Li, J. B. Wiley, D. Cimpoesu, A. Stancu, and L. Spinu, IEEE Trans. Magn. **41**, 3361 (2005).
[7] A. Encinas-Oropesa, M. Demand, L. Piraux, I. Huynen, and U. Ebels, Phys. Rev. B **63**, 104415 (2001).
[8] C. A. Ramos, M. Vazquez, K. Nielsch, K. Pirota, J. Rivas, R. B. Wehrspohn, M. Tovar, R. D. Sanchez, and U. Goesele, J. Magn. Magn. Mater. **272**, 1652 (2004).
[9] R. B. Marks, IEEE Trans. Microwave Theory Tech. **39**, 1205 (1991).
[10] B. Kuanr, L. Malkinski, R. Camley, Z. Celinski, and P. Kabos, J. Appl. Phys. **93**, 8591 (2003).
[11] R. Marson, B. K. Kuanr, S. R. Mishra, R. E. Camley, and Z. Celinski, J. Vac. Sci. Technol. B **25**, 2619 (2007).
[12] B. K. Kuanr, Y. Khivinitsev, A. Hutchison, R. E. Camley, and Z. Celinski, IEEE Trans. Magn. **43**, 2648 (2007).
[13] O. Acher, A. L. Adenot, F. Lubrano, and F. Duverger, J. Appl. Phys. **85**, 4639 (1999).
[14] O. Acher, A. L. Adenot, and F. Duverger, Phys. Rev. B **62**, 13748 (2000), and references therein.
[15] B. Kuanr, I. R. Harward, D. L. Marvin, T. Fal, R. E. Camley, D. L. Mills, and Z. Celinski, IEEE Trans. Magn. **41**, 3538 (2005).